

COMPARISON OF TRANSFER MAP DERIVATION METHODS FOR STATIC MAGNETIC FIELDS

J. A. Crittenden, S. Wang CLASSE, Cornell University, Ithaca NY 14853, USA

Abstract

We compare methods for deriving transfer maps for static magnetic fields, including field-map tracking and tracking elements defined by multipole content. Building on prior work on quantitative evaluation of the accuracy of finite-element models used to produce field maps, we assess the tradeoffs between computing time and fidelity to the underlying magnetic field, including fringe fields, of the various approximate methods. We illustrate our approach using the example of electromagnets in the south arc of the 6-GeV Cornell High Energy Synchrotron Source, which have been operating since 2019.

INTRODUCTION

The Cornell Electron-positron Storage Ring (CESR) underwent a major upgrade during 2018, when the south one-sixth of the ring, which formally hosted the CLEO detector, was replaced with a set of six double achromats [1]. Figure 1 shows a photo of one half of such an achromat cell. Two quadrupole magnets are shown, one of which is outfitted with an X-ray beam extraction channel.



Figure 1: Photograph of one half of the double achromat cell used in the 2018 upgrade of the south arc of the CESR ring.

Our investigations into using tracking algorithms in modeled field maps to improve the accuracy of the parameterized elements in the operations lattice centers in the present paper on the fully quadrupole-symmetric non-extraction version without the extraction channel. The accuracy of the field calculated using a finite element model has been described in detail in a recent publication [2]. One advantage of studying such a symmetric model is that the ability of the model to exclude multipole terms can be assessed, since certain terms are excluded by symmetry considerations, such as, in this case, sextupole and decapole terms. The finite-element

mesh used in this model which is implemented in the Opera simulation suite,¹ is shown in Fig. 2.

The result of the field calculation at nominal excitation is shown in Fig. 3 in the form of a color map of the magnetization field vector magnitude on the steel surfaces. Some evidence of saturation is visible in the pole tips.

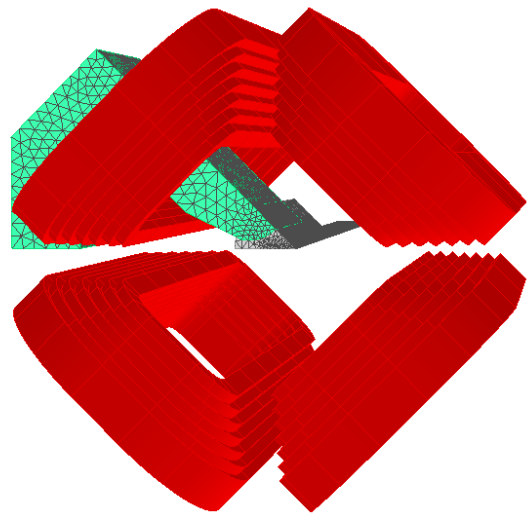


Figure 2: Finite-element mesh model implemented in Opera. The quadrupole symmetry allows for a one-sixteenth model. Nonetheless, numerical errors in the mesh can result in nonzero “forbidden” multipole coefficients.

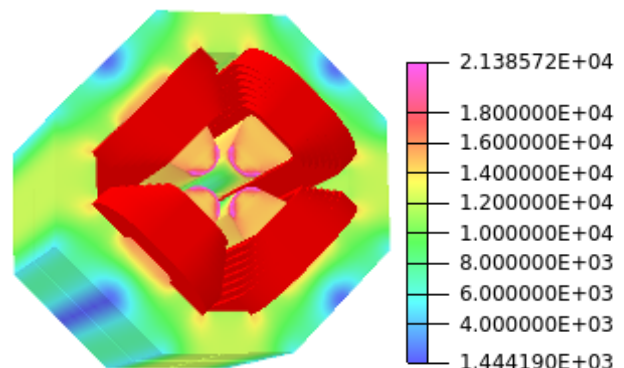


Figure 3: Color map of the magnetization field vector magnitude calculated in the Opera model for the non-extraction south arc quadrupole magnet at nominal field intensity. The units are Gauss. Some effects of saturation are evident in the pole tips.

¹ Opera Simulation Software Suite, Dassault Systèmes.

Content from this work may be used under the terms of the CC BY 3.0 licence (© 2021). Any distribution of this work must maintain attribution to the author(s), title of the work, publisher, and DOI

The present work on deriving transfer matrix elements from tracking through field maps obtained from finite-element models builds on earlier work on the assessment of the quality of such field maps [2]. Our tracking of the 6-GeV positrons is done using algorithms provided in the Bmad library [3].

MULTIPOLE ANALYSIS OF TRACKING RESULTS

To characterize the multipole content in the transport matrix element r_{21} we make a polynomial fit to the horizontal exit angle as a function of the horizontal entrance position. Skew multipole coefficients are thus ignored in this analysis. Figure 4 shows the result of Bmad tracking in the simple model used in the lattice for the non-extraction quadrupole magnet, which is parameterized solely by a field gradient and a length. The exit angle is translated to the trajectory-integrated vertical field component. The weights on the χ^2 -squared contributions have been adjusted to give $\chi^2/\text{NDF} \approx 1$, yielding a value for the weights of $5.33 \times 10^{-7} (\text{Tm})^{-2}$. All multipoles but for the quadrupole and dodecapole terms are found to be negligible within the uncertainties in the fit.

The effects of fringe fields on the transfer map elements can be obtained by tracking through discrete field maps, whereby the desired accuracy is limited by the accuracy of

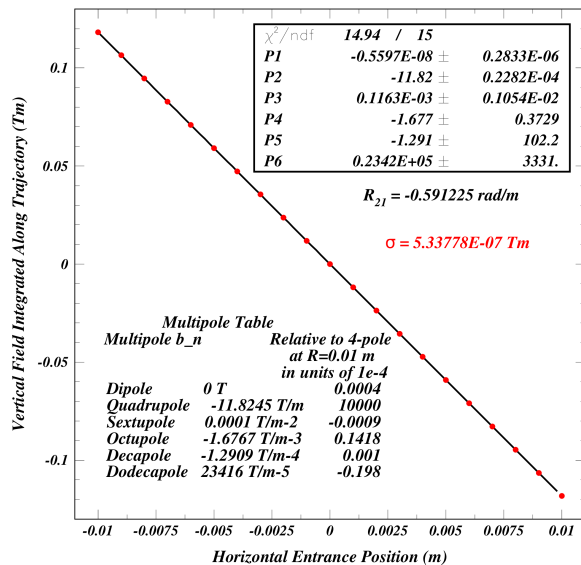


Figure 4: Multipole expansion for the horizontally defocusing transfer map element r_{21} giving the horizontal exit angle as a function of the horizontal entrance position, where the exit angle is expressed as the trajectory-integrated vertical magnetic field component in units of Tesla-meters. Skew multipoles are ignored in this analysis, since it is restricted to the horizontal mid-plane. This tracking analysis is done for the simple model for the non-extraction quadrupole magnet used in the design and operations lattice for CESR, consisting merely of values for the field gradient and length.

the finite-element model and the tracking algorithm. In our case, this technique revealed a significant dodecapole term $-2.776 \pm 0.024 \times 10^{-5} \text{ Tm/m}^{-5}$ in the multipole expansion of r_{21} . Figure 5 shows in blue the fit for the field-map tracking analogous to that for the simple model shown in Fig. 4, but now with the linear term subtracted for clarity. The linear-term-subtracted result for the simple model used in the lattice is superposed in black.

The Bmad library provides for lattice elements which can be defined using multipole coefficients derived from straight-line integrals in field maps. Figure 6 shows the result obtained from the finite-element model for the field map. Here the coefficients determined to have values smaller than their uncertainty have been suppressed to improve the accuracy in the determination of the observed dodecapole term. While it is determined to an accuracy of 1.7%, it is worthwhile noting that it is small by conventional magnet fabrication standards, 2 parts in 10^4 of the quadrupole term at a radius of 1 cm.

Having obtained the multipole coefficients in the field integrals, we apply them in the definition of the lattice element and use the Bmad tracking algorithm to determine the multipole content in r_{21} . The result with the linear term subtracted is shown as the red points in Fig. 7 together with the results shown in Fig. 5. We have thus obtained, to a certain accuracy, a model which is computationally fast, includes

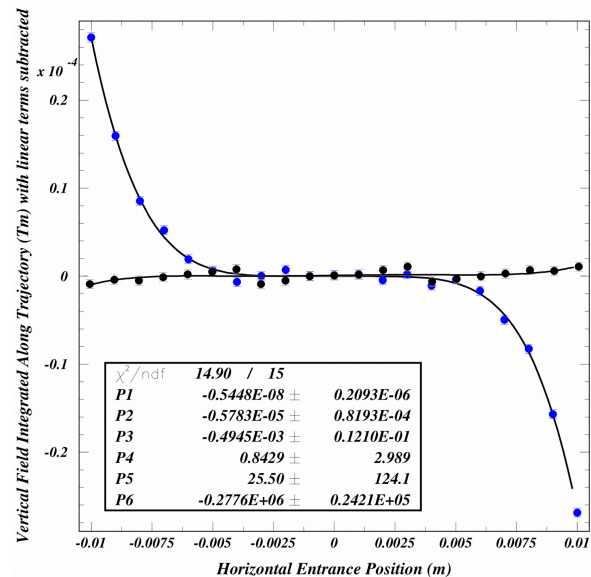


Figure 5: Multipole coefficients determined from Runge-Kutta tracking in the discrete field map. Here the linear term has been subtracted in order to emphasize the dodecapole term found in the field-map tracking (blue points). Superposed is the result from tracking in the simple model for the quadrupole presently implemented in the CESR lattice (black points), which is the same expansion as in Fig. 4, now with the linear term subtracted. The field-map tracking model finds a dodecapole term an order of magnitude larger and of opposite sign.

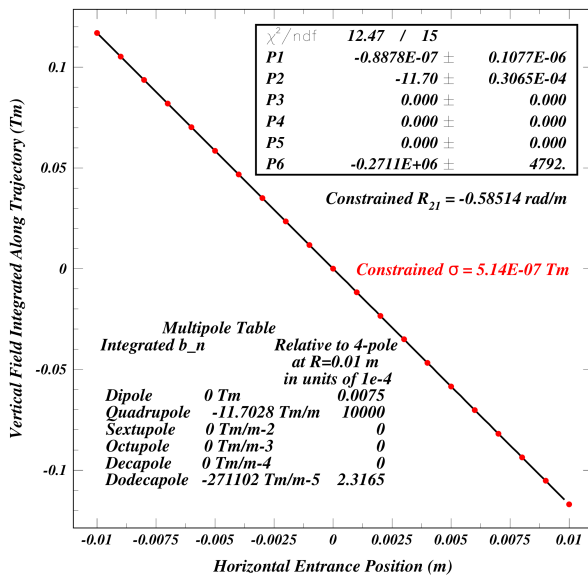


Figure 6: Multipole expansion of the straight-line integrals in the discrete field map. Coefficients less than their uncertainty in the unconstrained fit have now been constrained to zero to improve the accuracy in the determination of the significant dodecapole term. This coefficient can now be implemented in the lattice model for the magnet, providing a fast model which reproduces the multipole behavior observed in the field-map tracking shown in Fig. 5.

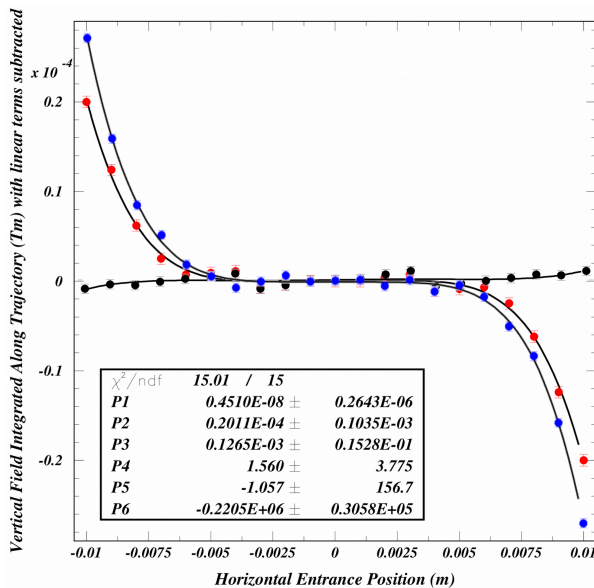


Figure 7: Result for the multipole expansion of the transport matrix element r_{21} in the model for the non-extraction quadrupole magnet which includes the dodecapole term identified in the multipole expansion of the straight-line field integrals in the field map, shown as the red points. The results for the initial simple model (black) and the field-map tracking (blue) are included for comparison. A dodecapole term is found which is similar to that found for the field-map tracking. This is now a model which is computationally fast and includes the effects of the fringe fields.

the fringe field effects, and reproduces the multipole content observed in the field-map tracking result.

SUMMARY

We are investigating various approximate methods to produce transfer maps from finite-element models of magnetostatic fields. Using the example of the quadrupole magnets in the south arc upgrade of CESR for the Cornell High-energy Synchrotron Source, we developed finite-element models for the field and compared tracking in the field map to tracking in the simple model presently implemented in the design and operations lattice model, using tracking algorithms provided in the Bmad library. We obtained a model which is computationally fast and reproduces the multipole content of the field map for the transfer matrix element r_{21} .

We plan further investigations into tracking algorithms implemented in the Bmad library, such as Taylor maps and polymorphic tracking code. The above studies for the matrix element r_{21} can obviously be extended to the other transfer matrix elements.

These methods will be particularly useful for magnets with high multipole content due to, for example, severe space constraints on the design, such as was the case for the Cornell-Brookhaven Energy-recovery-linac Test Accelerator [4, 5].

ACKNOWLEDGMENTS

This work is supported by National Science Foundation award numbers DMR-1829070 and PHY-1757811.

REFERENCES

- [1] J. Shanks *et al.*, “Accelerator design for the Cornell High Energy Synchrotron Source upgrade”, *Phys. Rev. Accel. Beams*, vol. 22, p. 021602, 2019.
doi:10.1103/PhysRevAccelBeams.22.021602
- [2] J. A. Crittenden, “Quantitative assessment of finite-element models for magnetostatic field calculations”, *Nucl. Instrum. Meth. A*, vol. 1005, p. 165370, 2021.
doi:10.1016/j.nima.2021.165370
- [3] D. Sagan, “Bmad: A relativistic charged particle simulation library,” in *Proc. ICAP’04*, St. Petersburg, Russia, Jun.-Jul. 2004, *Nucl. Instrum. Meth. A*, vol. A558, pp. 356–359, 2006.
doi:10.1016/j.nima.2005.11.001
- [4] A. Bartnik *et al.*, “CBETA: First Multipass Superconducting Linear Accelerator with Energy Recovery”, *Phys. Rev. Lett.*, vol. 125, p. 044803, 2020.
doi:10.1103/PhysRevLett.125.044803
- [5] J. A. Crittenden *et al.*, “Initial Performance of the Magnet System in the Splitter/Combiner Section of the Cornell-Brookhaven Energy-Recovery Linac Test Accelerator”, in *Proc. 9th Int. Particle Accelerator Conf. (IPAC’18)*, Vancouver, Canada, Apr.-May 2018, pp. 2986–2989. doi:10.18429/JACoW-IPAC2018-THPAF019